Clinical & Experimental Immunology
The Journal of Translational Immunology
British Society for immunology

Clinical and Experimental Immunology ORIGINAL ARTICLE doi:10.1111/cei.12137

Impaired removal of Vβ8$^+$ lymphocytes aggravates colitis in mice deficient for B cell lymphoma-2-interacting mediator of cell death (Bim)

K. Leucht, M. Caj, M. Fried, G. Rogler and M. Hausmann
Division of Gastroenterology and Hepatology, Department of Internal Medicine, University Hospital of Zürich, Zürich, Switzerland

Accepted for publication 7 May 2013
Correspondence: M. Hausmann, Division of Gastroenterology and Hepatology, Department of Internal Medicine, University Hospital of Zürich, Raemistrasse 100, 8091 Zurich, Switzerland.
E-mail: martin.hausmann@usz.ch

Summary

We investigated the role of B cell lymphoma (BCL)-2-interacting mediator of cell death (Bim) for lymphocyte homeostasis in intestinal mucosa. Lymphocytes lacking Bim are refractory to apoptosis. Chronic colitis was induced in *Bim*-deficient mice (*Bim*$^{-/-}$) with dextran sulphate sodium (DSS). Weight loss and colonoscopic score were increased significantly in *Bim*$^{-/-}$ mice compared to wild-type mice. As Bim is induced for the killing of autoreactive cells we determined the role of Bim in the regulation of lymphocyte survival at mucosal sites. Upon chronic dextran sulphate sodium (DSS)-induced colitis, *Bim*$^{-/-}$ animals exhibited an increased infiltrate of lymphocytes into the mucosa compared to wild-type mice. The number of autoreactive T cell receptor (TCR) Vβ8$^+$ lymphocytes was significantly higher in *Bim*$^{-/-}$ mice compared to wild-type controls. Impaired removal of autoreactive lymphocytes in *Bim*$^{-/-}$ mice upon chronic DSS-induced colitis may therefore contribute to aggravated mucosal inflammation.

Keywords: apoptosis, autoreactive TCR, Bim, Vβ8$^+$ lymphocytes

Introduction

Pro-survival B cell lymphoma (BCL)-2 interacts with pro-apoptotic BCL-2-interacting mediator of cell death (Bim). Bim is sequestered to microtubules [1], by which Bim can be separated from BCL-2. Upon apoptotic stimuli, such as ultraviolet (UV) irradiation and growth factor withdrawal, Bim translocates to BCL-2 and neutralizes its anti-apoptotic activity. This process does not require caspase activity, and therefore constitutes an initiating event in apoptosis signalling. Bim was suggested to have an increased prevalence of phosphorylation sites. Bim is phosphorylated and targeted for degradation by the proteasome [2].

Inactivation of BCL-2 has been suggested to be the key to the ability of Bim to induce apoptosis. However, an alternative model argues that some forms of Bim can also bind directly to the other pro-apoptotic proteins Bax and Bak in order to initiate apoptosis [3]. Bax and Bak act by forming pores in the mitochondrial membrane, finally triggering apoptosis. Other BH3-only proteins, such as Bmf, Bad, Noxa and Puma, are considered to act as sensitizers which bind the pro-survival BCL-2 protein and thereby displace Bim from BCL-2 to promote cell death [4].

Bim transduces death signals not only after its release from the actin cytoskeleton, but also by activation of its transcription. *Bim* transcription is induced by transforming growth factor (TGF)-β-driven apoptosis in a number of cell types [5]. TGF-β-induced autophagy potentiates the induction of the pro-apoptotic Bim by the stress-responsive transcription factor C/EBP homologous protein (CHOP) upon growth factor withdrawal [6].

Bcl-2 and Bim play a critical role in the establishment and maintenance of the immune system by regulating the survival of lymphocytes by apoptosis. The effect of the interaction of Bcl-2 and Bim is dependent on the cell type and/or is tissue-specific: Bcl-2 promotes the survival of naive T cells [7]. In turn, naive T cells from *Bim*$^{+/-}$ *Bcl-2*$^{-/-}$ mice die at an accelerated rate *in vitro*. Bcl-2 is critical to prevent the pro-apoptotic effects of Bim in naive CD8$^+$ T cells *in vivo*, but other molecules than Bcl-2 might antagonize Bim in CD4$^+$ cells. Bim controls T cell numbers in the periphery by promoting apoptosis and/or decreasing thymic production. Bim-deficient mice have elevated numbers of normal single-positive T cells in the periphery [8]. Bim is a primary trigger for killing autoreactive B cells during their development [9]. In contrast, Bcl-2 is required less for the generation and/or maintenance of memory T cells [7].

Bcl-2 and Bim play a critical role in controlling immune responses by regulating the survival, expansion and con-

traction of lymphocytes by apoptosis. The majority of activated T cells die at the end of a T cell response. Activated T cells exhibit decreased levels of Bcl-2 at the peak of the T cell response, just before they began to die *in vivo* [10]. A decrease of the pro-survival protein Bcl-2 contributes to apoptosis of activated T cells [11]. Bim deficiency prevents the death of activated T cells *in vitro* and *in vivo*, suggesting that the protective effects of Bcl-2 acts solely to neutralize Bim [11].

Thymocytes can be selected negatively by exposure to anti-CD3 antibody, which aggregates the TCR–CD3 complex and kills the $CD4^+CD8^+$ population *in vivo* and *in vitro*. Thymocytes lacking the pro-apoptotic Bim are refractory to TCR ligation-induced killing [12]. Stimulation with the superantigen *Staphylococcus* enterotoxin B (SEB) activates most T cells that express a variable region (V)-β8 TCR. Addition of SEB to fetal thymic organ cultures deletes most developing TCR $V\beta8^+$ thymocytes. In contrast, TCR $V\beta8^+$ escapes apoptosis in SEB-treated thymic lobes from *Bim*$^{-/-}$ embryos [12].

Lymphocytes from *Bim*$^{-/-}$ mice were found to be relatively resistant to apoptosis upon BH3-only mimetics compared to those from wild-type mice. The presence of Bim affected apoptosis of regulatory T cells (T_{reg}) differently when compared to $CD4^+8^-$ thymocytes. The loss of pro-apoptotic Bim rescued T_{reg} cells from intrinsically initiated apoptosis [13]. As well as the role of Bim for apoptosis of T_{reg} cells, the absence of Bim also affects the phenotype and function of T_{reg} cells in a manner that indicates loss of function.

An exaggerated response of T lymphocytes to luminal antigens is suggested to increase intestinal inflammation in inflammatory bowel disease (IBD). In Crohn's disease (CD), mucosal T cells escape normal apoptosis. The lifespan of antigen-primed T cells is extended and an abnormal population of activated cells is retained within the mucosal compartment.

Enhanced expression of the pro-survival proteins BCL-2 and BCL-x_L were determined in lamina propria T cells of patients with CD compared to controls. Lamina propria T cells in CD show activation of the signal transducer and activator of transcription (STAT)-3 signalling pathway mediated by interleukin (IL)-6. Activation of STAT-3 is followed by the induction anti-apoptotic genes such as *BCL*-2 and *BCL*-x_L [14]. Resistance of CD T cells to multiple apoptotic signals is associated with increased BCL-2 expression. An abnormal BCL-2 expression in lamina propria mononuclear cells from patients with CD was demonstrated [15]. A significantly higher BCL-2/Bax ratio in CD mucosa compared to control was reported [16]. These data are consistent with a recent report showing significant resistance to Fas-induced apoptosis of peripheral T cells from CD patients [17]. However, no significant difference was reported in the BCL-2/Bax ratio in peripheral blood from CD patients compared to control.

Our own studies on apoptosis of lymphocytes in the gut mucosa revealed that cell death in Peyer's patches is dependent upon the pro-apoptotic protein BIM. Based on these findings we investigated the role of Bim for cell death of lymphocytes in mice under inflammatory conditions.

Material and methods

Induction and treatment of chronic dextran sulphate sodium (DSS) colitis

B6.129-Bcl2l11$^{tm1.1Ast}$/J (*Bim*$^{-/-}$) mice were kindly provided by Professor Dr Andreas Villunger (Division for Developmental Immunology, Innsbruck Medical University). *Bim*$^{-/-}$ mice were back-crossed for at least 12 generations [18]. Mice weighing 20–25 g were used for the experiments and housed in individually ventilated cages (IVC). All animals were housed for at least 3 weeks prior to testing in a specific pathogen-free (SPF) facility. Chronic colitis was induced as described previously [19]. During a cycle of chronic colitis, mice received either 2·5% DSS in drinking water or drinking water alone over 7 days. In between, the animals were given 14-day periods of recovery. Female mice received three to five cycles of DSS treatment as described. Mice were killed 2 weeks after completion of the last DSS cycle.

Assessment of colonoscopy and histological score in mice

Animals were anaesthetized intraperitoneally (i.p.) with a mixture of 90–120 mg ketamine (Narketan 10%; Vétoquinol AG, Bern, Switzerland) and 8 mg xylazine (Rompun 2%; Bayer, Basel, Switzerland) per kg body weight and examined with the Tele Pack Pal 20043020 (Karl Storz Endoskope, Tuttlingen, Germany) and scored with a murine endoscopic index of colitis severity (MEICS), as described previously [20].

Assessment of histological score in mice

For the assessment of the histological scores, 1 cm of the distal third of the colon was removed and scored as described [19,21].

RNA extraction and quantitative real-time polymerase chain reaction (PCR)

Total RNA was extracted from murine tissue using the RNeasy Mini Kit and the automated sample preparation system QIAcube, as proposed by the manufacturer (Qiagen, Basel, Switzerland). mRNA was reverse-transcribed into cDNA using a high-capacity cDNA reverse transcription kit (Applied Biosystems, Foster City, CA, USA). *Bim* and *iNos* gene expression was determined with a *Taq*Man® Gene

Expression Assay (#Mm00437796_m1 and #Mm01309893_m1; Applied Biosystems). Glyceraldehyde 3-phosphate dehydrogenase (GAPDH) gene expression was measured as endogenous control (#4352339E; Applied Biosystems) and used for calculation of relative mRNA expression by the ΔΔCt method. All samples were analysed in triplicate.

Western blot

Samples were lysed in mammalian protein extraction reagent (M-PER) protein extraction buffer (Thermo Fisher Scientific, Perbio Science, Lausanne, Switzerland). Proteins were separated on 10% polyacrylamide gels with Tris/sodium dodecyl sulphate (SDS) running buffer and transferred onto nitrocellulose (Invitrogen, Carlsbad, CA, USA). Membranes were blocked with 5% milk, 3% bovine serum albumin (BSA) and 0·1% Tween 20 and incubated with rabbit anti-mouse inducible nitric oxide synthase (iNOS) (#2977S; Cell Signalling, Inc., Danvers, MA, USA); the horseradish peroxidase-conjugated secondary antibody was goat anti-rabbit (#sc-2004; Santa Cruz Biotechnology, Inc., Santa Cruz, CA, USA; diluted 1 : 3000). β-actin was used as a loading control.

Immunofluorescence (IF)

Murine colonic tissue samples were fixed in 3·7% formaldehyde, embedded in paraffin and cut. Demasking for TCR Vβ8 IF was performed using Dako target retrieval solution (# S2367, pH 9) and proteinase K (Dako, Glostrup, Denmark); 1% BSA in PBS was used to block unspecific binding sites. Primary antibodies were fluorescein isothiocyanate (FITC)-labelled mouse anti-mouse TCR Vβ8 (# BD 553861; BD Biosciences, San Jose, CA, USA). Nuclei were visualized with diamidino phenylindole (DAPI; Invitrogen; final concentration 3 μM). The sections were mounted with fluorescent mounting medium (Dako) and analysed by confocal laser scanning microscopy (SP5; Leica, Heerbrugg, Switzerland).

Statistical analysis

Real-time PCR data were calculated from triplicates. Statistical analyses were performed using PASW statistics version 18.0 (SPSS Inc., Chicago, IL, USA). The Kruskal–Wallis non-parametric analysis of variance and Bonferroni-corrected Mann–Whitney rank sum test were applied for animal experiments. Box-plots express median, 25% quartiles around median, minimum and maximum. One-way analysis of variance (ANOVA) and Tukey's *post hoc* test were used for cell culture experiments. Bars represent mean values with whiskers displaying standard deviation. Differences were considered significant at $P < 0{\cdot}05$ (*), highly significant at $P < 0{\cdot}01$ (**) and very highly significant at $P < 0{\cdot}001$ (***). Luminescence Western blot was quantified densitometrically with OptiQuant (Packard Instruments, Meriden, CT, USA).

Ethical considerations

The experimental protocol was approved by the local Animal Care Committee of the University of Zurich (146/2009) and was granted by the Swiss National Science Foundation (SNF 31003A_127247) to M. Hausmann and the Broad Medical Research Foundation (IBD-0324) to M. Hausmann.

Results

Bim$^{-/-}$ mice develop rectum prolapses

Previous experimental evidence has indicated that the loss of *Bmf* causes defects in uterovaginal development, e.g. an imperforate vagina and hydrometrocolpos [22]. We analysed phenotypic abnormalities of *Bim*$^{-/-}$ animals in the anal canal. Animals were kept in IVC under SPF conditions. Rectum prolapses were found in 18 of 104 *Bim*$^{-/-}$ animals (Fig. 1a,b) which have not been used for breeding; anal bleeding was observed in those mice. No increase in collagen deposition in *Bim*$^{-/-}$ colon was detectable by Sirius red and Elastica von Giesson staining (not shown). Analysis of the length of collagen fibrils by polarized light microscopy also revealed no change in *Bim*$^{-/-}$ animals with prolapse compared to wild-type mice without prolapse. Colon length was not altered in *Bim*$^{-/-}$ animals compared to wild-type mice ($8{\cdot}0 \pm 1{\cdot}0$, $n = 18$ *versus* $7{\cdot}9 \pm 0{\cdot}8$, $n = 15$, respectively, not shown). Transepithelial resistance was measured at a 1–2 cm distance from the distal end of the colon. Transepithelial resistance was not altered in *Bim*$^{-/-}$ animals compared to wild-type mice ($35 \pm 5\ \Omega \times cm^2$, $n = 5$ *versus* $39 \pm 6\ \Omega \times cm^2$, $n = 5$, respectively, female mice without rectum prolapse, not shown).

Previous experimental evidence has reported impaired cell death of lymphocytes in the absence of Bim [18]. We analysed peripheral blood from seven wild-type controls and seven Bim$^{-/-}$ mice on an ADVIA 2120i haematology system (Siemens AG, Munich, Germany). The total number of leucocytes was increased significantly in Bim$^{-/-}$ mice compared to wild-type controls ($8{\cdot}21 \pm 2{\cdot}52 \times 10^9$ cells/l *versus* $1{\cdot}66 \pm 0{\cdot}48 \times 10^9$ cells/l, $P < 0{\cdot}001$). Total numbers of lymphocytes ($6{\cdot}61 \pm 2{\cdot}90 \times 10^3$ cells/μl *versus* $1{\cdot}24 \pm 0{\cdot}34 \times 10^3$ cells/μl, $P < 0{\cdot}001$), neutrophilic leucocytes ($1{\cdot}20 \pm 1{\cdot}27 \times 10^3$ cells/μl *versus* $0{\cdot}28 \pm 0{\cdot}25 \times 10^3$ cells/μl, $P < 0{\cdot}001$) and eosinophilic leucocytes ($0{\cdot}24 \pm 0{\cdot}20 \times 10^3$ cells/μl *versus* $0{\cdot}06 \pm 0{\cdot}03 \times 10^3$ cells/μl, $P < 0{\cdot}001$) were increased significantly in Bim$^{-/-}$ mice compared to wild-type controls. In contrast, the proportion of monocytes was decreased significantly in Bim$^{-/-}$ mice compared to wild-type controls ($0{\cdot}91 \pm 0{\cdot}30$ *versus* $2{\cdot}73 \pm 1{\cdot}24$, $P < 0{\cdot}001$).

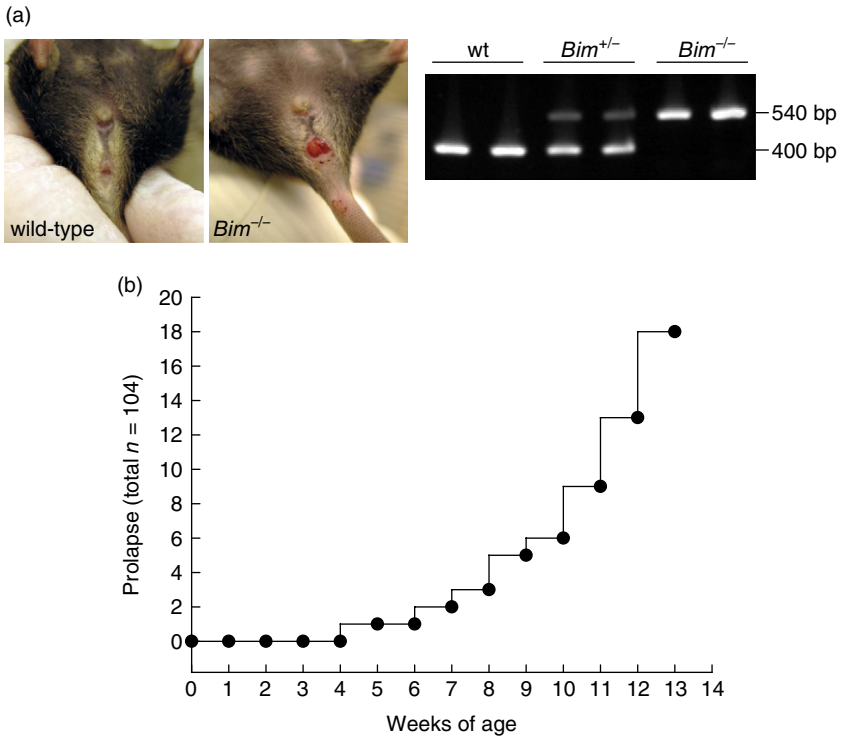

Fig. 1. *Bim*$^{-/-}$ mice developed anal bleeding and rectum prolapses spontaneously. (a) Prolapse in *Bim*$^{-/-}$ mice. Genotyping of *Bim*$^{-/-}$ mice. (b) Quantification of prolapses.

Consistently, we observed a significant difference in the spleen weight between *Bim*$^{-/-}$ and wild-type mice (spleen weight/body weight $7{\cdot}7 \pm 0{\cdot}9$ mg/g, $n = 10$ *versus* $4{\cdot}2 \pm 0{\cdot}4$ mg/g, $n = 5$; respectively, $P < 0{\cdot}05$, Fig. 3a).

Intestinal inflammation is aggravated in *Bim*$^{-/-}$ mice upon chronic DSS-colitis

As we found rectum prolapses, anal bleeding and a significant increase in the spleen weight in our *Bim*$^{-/-}$ animals, we focused on Bim dependence of intestinal inflammation and lymphocyte apoptosis in chronic DSS-induced colitis. Upon chronic DSS-induced colitis, the weight loss of *Bim*$^{-/-}$ mice was significantly higher compared to wild-type mice during the last days before the animals were killed (Fig. 2a). The macroscopic mucosal damage was assessed by colonoscopy and MEICS [20]. Mucosa from female *Bim*$^{-/-}$ mice and wild-type mice without colitis displayed a smooth and transparent mucosa with a normal vascular pattern ($0{\cdot}4 \pm 0{\cdot}4$, $n = 7$ *versus* $0{\cdot}2 \pm 0{\cdot}4$, $n = 5$ respectively; not shown). After induction of chronic colitis the colons of both *Bim*$^{-/-}$and wild-type mice appeared with an opaque, thickened, more granular mucosa and an altered vascular pattern. *Bim*$^{-/-}$ animals exhibited significantly higher MEICS score compared to wild-type mice ($5{\cdot}1 \pm 1{\cdot}7$, $n = 7$ *versus* $2{\cdot}7 \pm 1{\cdot}8$, $n = 5$ respectively; Fig. 2b).

Spleens of healthy wild-type mice were significantly smaller than those of *Bim*$^{-/-}$ animals. Upon DSS, the spleen weight increased significantly in wild-type animals ($P < 0{\cdot}05$) and highly significantly in *Bim*$^{-/-}$ animals ($P < 0{\cdot}01$, Fig. 3a). Induction of chronic colitis was followed by a typical reduction of colon length. Shortening of the colon was significant in DSS-receiving *Bim*$^{-/-}$ animals compared to the respective controls ($8{\cdot}1 \pm 0{\cdot}5$ cm upon water, $n = 5$, *versus* $7{\cdot}0 \pm 0{\cdot}8$ cm upon DSS, $n = 5$ for wild-type animals. $8{\cdot}8 \pm 0{\cdot}4$ cm upon water, $n = 7$, *versus* $7{\cdot}8 \pm 0{\cdot}5$ cm upon DSS, $n = 7$, $P < 0{\cdot}05$ for *Bim*$^{-/-}$ mice; Fig. 3b). Increase of spleen weight upon chronic DSS-induced colitis correlated with a decrease in colon length for both wild-type controls and *Bim*$^{-/-}$ mice ($P < 0{\cdot}05$). Combining data from wild-type controls and *Bim*$^{-/-}$ mice upon both water and DSS, no significant relationship between spleen weight and colon length could be determined because of the significant difference in the spleen weight between wild-type and *Bim*$^{-/-}$ in mice without inflammation.

Also on a microscopic level, more severe colitis was found for *Bim*$^{-/-}$ mice compared to wild-type mice. In female animals without chronic DSS-induced colitis, the *Bim* knock-out did not alter the total histological score compared to the wild-type ($1{\cdot}2 \pm 0{\cdot}6$ *versus* $1{\cdot}3 \pm 0{\cdot}6$, respectively; Fig. 3c). The total histological score for *Bim*$^{-/-}$ mice with induced chronic colitis was increased significantly compared to the water-treated mice. The score for epithelial damage considering crypt morphology and loss of goblet cells remained unchanged when comparing DSS-receiving *Bim*$^{-/-}$ and wild-type mice (Fig. 3c, white bars). In contrast, *Bim*$^{-/-}$ animals with chronic colitis exhibited a significantly increased inflammatory infiltrate of lymphocytes into the mucosa and submucosa compared to wild-type mice ($4{\cdot}4 \pm 0{\cdot}8$ *versus* $3{\cdot}1 \pm 1{\cdot}0$, respectively; $P < 0{\cdot}05$; Fig. 3c,

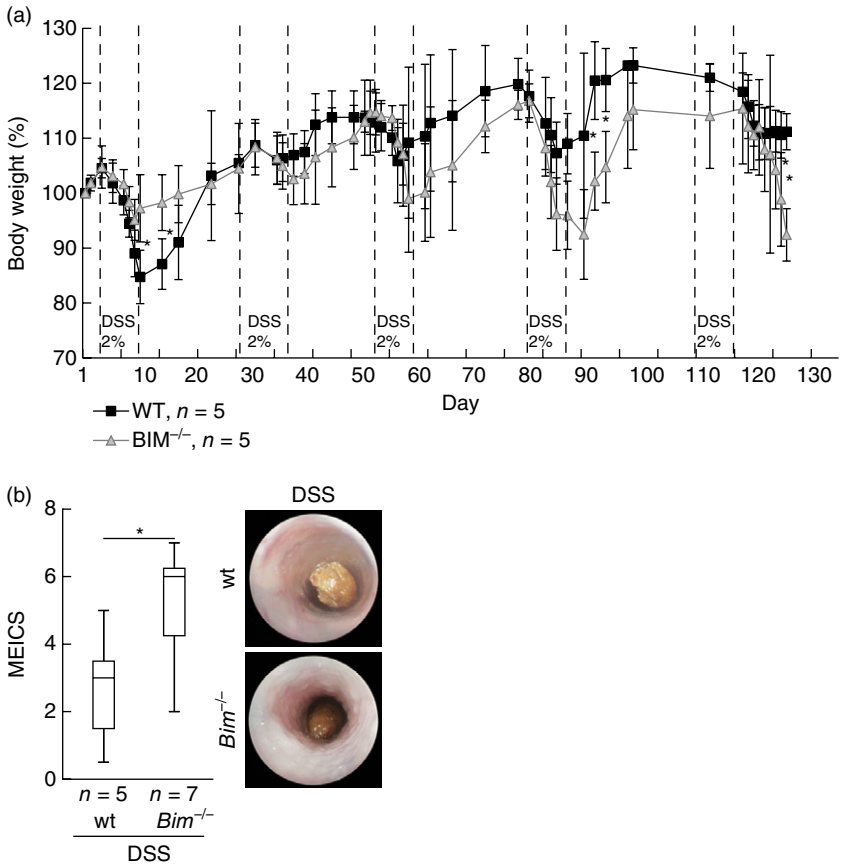

Fig. 2. *Bim*$^{-/-}$ mice develop an aggravated chronic dextran sulphate sodium (DSS)-induced colitis compared to wild-type (wt) mice. (a) Percentage body weight loss [± standard deviation (s.d.)]. (b) Statistical analysis of colonoscopy score [murine endoscopic index of colitis severity (MEICS)]. Colonoscopy was performed on the day prior to euthanizing the animals. Representative images demonstrate colonoscopy pictures derived from DSS-treated wt mice and *Bim*$^{-/-}$ mice. $^{*}P < 0{\cdot}05$.

light grey bars). This also led to a significantly higher total histological score for *Bim*$^{-/-}$ mice with chronic colitis compared to wild-type mice ($6{\cdot}7 \pm 1{\cdot}4$ *versus* $4{\cdot}9 \pm 0{\cdot}4$ respectively; $P < 0{\cdot}05$; Fig. 3c, dark grey bars).

The results were confirmed in a second experiment of chronic DSS-induced colitis in female mice ($n = 5$ each group, not shown). In a third experiment in male *Bim*$^{-/-}$ mice, similar data were obtained ($n = 5$ each group, not shown). In these animals, more severe inflammation for *Bim*$^{-/-}$ animals compared to wild-type mice was determined upon chronic DSS-induced colitis.

Impaired removal of autoreactive lymphocytes in *Bim*$^{-/-}$ mice upon chronic DSS-induced colitis contributes to aggravated mucosal inflammation

As lymphocyte killing is impaired in *Bim*$^{-/-}$ mice and loss of function is indicated for T_{regs} from those animals, we focused on the induction of apoptosis in lymphocytes in chronic DSS-induced colitis in *Bim*$^{-/-}$ animals compared to wild-type mice. The histological score shows a significantly increased lymphocyte infiltration in the intestinal mucosa in *Bim*$^{-/-}$ animals compared to wild-type animals upon chronic DSS-induced colitis.

First, we isolated Peyer's patches by excising whole lymph nodes together with adherent mucosal tissue. We could show increased gene expression levels for *Bim* in wild-type mice when they had developed chronic colitis (control: $1{\cdot}1 \pm 0{\cdot}3$, $n = 5$; DSS: $1{\cdot}5 \pm 0{\cdot}6$, $n = 5$; Fig. 3d).

As TCR Vβ8^{+} T cells from *Bim*$^{-/-}$ mice were found to be resistant to enterotoxin-induced deletion [11], and apoptosis of TCR Vβ8^{+} T cells but not TCR Vβ6^{+} T cells is impaired in *Bim*$^{-/-}$ mice [12], we focused on the presence of TCR Vβ8^{+} T cells in Peyer's patches by flow cytometric analysis. The number of TCR Vβ8^{+} lymphocytes was increased significantly in Peyer's patches from *Bim*$^{-/-}$ mice compared to wild-type controls ($10{\cdot}5 \pm 1{\cdot}9\%$ *versus* $7{\cdot}3 \pm 1{\cdot}2\%$, respectively, $P < 0{\cdot}05$; Fig. 4a). An increase of TCR Vβ8^{+} lymphocytes was confirmed by IF for *Bim*$^{-/-}$ mice compared to wild-type controls (Fig. 4b).

The cytokine profile of mucosal lymphocytes is altered in *Bim*$^{-/-}$compared to wild-type mice

Whole Peyer's patches were excised and snap-frozen. We assessed the cytokine profile in whole Peyer's patches without further pre-stimulation of lymphocytes on the level of mRNA. *iNos* gene expression was detectable in wild-type but almost absent in *Bim*$^{-/-}$ animals without chronic colitis ($1{\cdot}10 \pm 1{\cdot}00$, $n = 9$ *versus* $0{\cdot}34 \pm 0{\cdot}24$, $n = 12$, respectively, Fig. 5a). There was a significant difference for wild-type mice upon chronic DSS-induced colitis compared to *Bim*$^{-/-}$

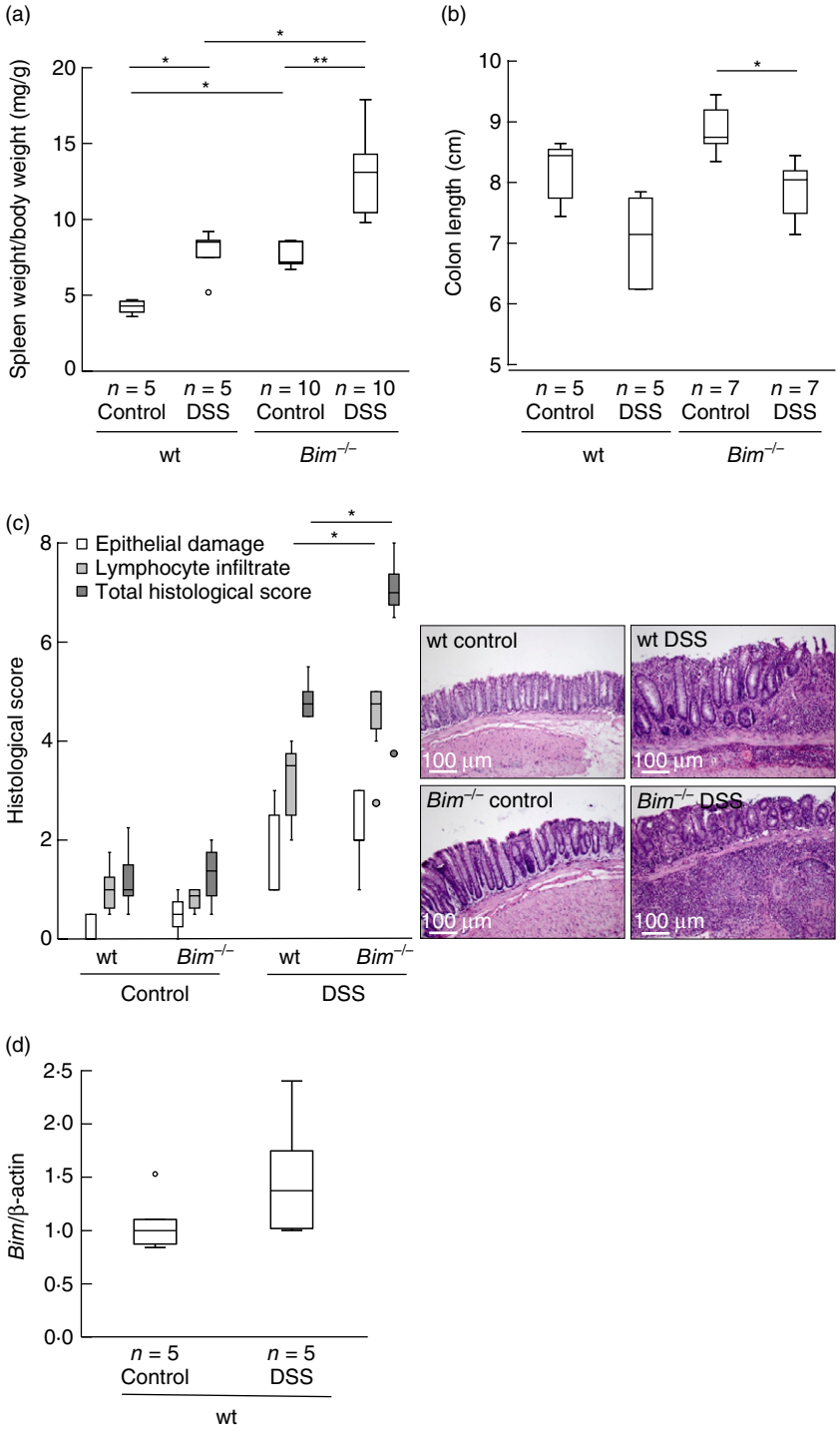

Fig. 3. *Bim*$^{-/-}$ mice develop an aggravated chronic dextran sulphate sodium (DSS)-induced colitis. (a) Statistical analysis of spleen weight per body weight. (b) Statistical analysis of colon length and representative images. (c) Histoscore derived from water- ($n = 4$) or DSS-treated ($n = 5$) wild-type (wt) and water- ($n = 7$) or DSS-treated ($n = 7$) *Bim*$^{-/-}$ mice. (d) *Bim* is increased in Peyer's patches in wt mice upon chronic DSS. *$P < 0{\cdot}05$; **$P < 0{\cdot}01$.

animals ($1{\cdot}00 \pm 0{\cdot}97$, $n = 15$ *versus* $0{\cdot}23 \pm 0{\cdot}14$, $n = 17$, respectively, $P < 0{\cdot}05$; Fig. 5a). Data could be confirmed by Western blot. Wild-type mice exhibited significantly higher iNOS protein contents than *Bim*$^{-/-}$ mice for animals both with and without chronic DSS-induced intestinal inflammation ($0{\cdot}18 \pm 0{\cdot}04$, $n = 3$, *versus* $0{\cdot}02 \pm 0{\cdot}03$, $n = 5$, respectively, for mice without DSS-induced chronic colitis and $0{\cdot}12 \pm 0{\cdot}08$, $n = 7$, *versus* $0{\cdot}02 \pm 0{\cdot}05$, $n = 6$, $P < 0{\cdot}05$, respectively, for mice with DSS-induced chronic colitis; Fig. 5b). For *IL-6*, *TNF* and *IL-1*β mRNA expression, no significant changes were recorded between wild-type and *Bim*$^{-/-}$ mice with and without chronic DSS-induced colitis (not shown).

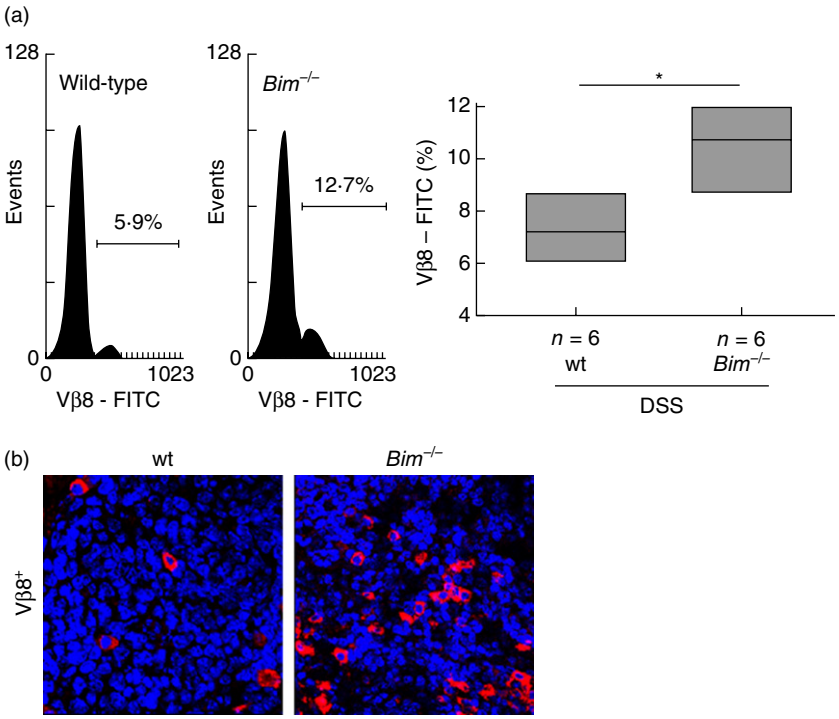

Fig. 4. Impaired removal of autoreactive lymphocytes in Bim$^{-/-}$ upon chronic dextran sulphate sodium (DSS)-induced colitis. (a) Flow-cytometric analysis of T cell receptor (TCR) Vβ8^{+} lymphocytes isolated from murine Peyer's patches and statistical analysis; TCR Vβ8^{+} lymphocytes are shown as percentage of the total number of isolated cells (*$P < 0{\cdot}05$, Bonferroni's *t*-test, $n = 6$ each). (b) Immunofluorescence for TCR Vβ8^{+} in sections from Peyer's patches from wild-type (wt) and *Bim*$^{-/-}$.

Discussion

Bim interacts with the pro-survival family member BCL-2. Bim is involved critically in negative selection of thymocytes during maturation processes and Bim plus Puma co-regulate lymphocyte homeostasis in the periphery [9]. Deletion of activated cells after antigenic challenge is impaired in Bim-deficient animals, thereby facilitating the development of systemic lupus erythematosus-like pathology [8]. As dysregulated apoptosis of lymphocytes contributes to the pathogenesis of IBD [14–17,23], we analysed the role of Bim in lymphocytes in our mouse model of colitis.

In the present study, we show an impaired removal of autoreactive lymphocytes in *Bim*$^{-/-}$ mice upon chronic DSS-induced colitis. The presence of a significantly increased number of TCR Vβ8^{+} lymphocytes in Peyer's patches upon chronic DSS-induced colitis is associated with aggravated mucosal inflammation, as determined by significantly increased weight loss and MEICS score of *Bim*$^{-/-}$ compared to wild-type mice. Data from spleen weight, colon length and histological score confirmed this suggestion. Interestingly, TCR Vβ8^{+} lymphocytes can bind SEB. Wild-type mice treated with a single intrarectal instillation of SEB displayed a time- and dose-dependent colonic inflammation which was further increased significantly in ovalbumin transgenic mice with 95% TCR Vβ8^{+} lymphocytes [24].

Enhanced expression of the pro-survival proteins BCL-2 and BCL-x_L was determined in lamina propria T cells of patients with CD when compared with controls. Lamina propria T cells in CD patients show activation of the STAT-3 signalling pathway mediated by IL-6. Activation of STAT-3 is followed by the induction of anti-apoptotic genes such as *BCL*-2 and *BCL*-x_L [14]. Resistance of CD T cells to multiple apoptotic signals is associated with increased BCL-2 expression. An abnormal BCL-2 expression in lamina propria mononuclear cells from patients with CD was demonstrated [15]. A significantly higher BCL-2/Bax ratio in CD mucosa compared to controls was reported [16]. These data are consistent with a recent report showing significant resistance to Fas-induced apoptosis of peripheral T cells from CD patients [17]. The same immunological consequence resulting from the extended lifespan of antigen-primed T cells is supported by a reduced survival or function of T_{reg} cells. Apoptosis is elevated strongly in mucosal and peripheral CD4^{+}CD25^{high}forkhead box protein 3 (FoxP3)$^{+}$ T_{reg} cells of patients with IBD [25]. Failure of the apoptotic mechanism of lymphocyte control can lead to the development of autoimmunity or lymphoma.

Bim deficiency perturbed thymic T cell development. As expected for the loss of a pro-apoptotic molecule, the numbers of both the CD4^{-}8^{-} pro-T cells and the mature T cells (CD4^{+}8^{-} and CD4^{-}8^{+}) were two- to threefold higher than in wild-type animals. Surprisingly, however, the CD4^{+}8^{+} pre-T cells, the predominant thymic subpopulation, were only half the normal level [8].

Interestingly, we observed rectum prolapses in *Bim*$^{-/-}$ animals. The trigger for the appearance of prolapses was not investigated in this work. As described for mice homozygous for *Il10*^{tm1Cgn}, targeted mutations leading to altered lymphocyte populations are most likely to be involved in prolapse formation. As described for IL-10$^{-/-}$ mice, animal housing conditions and the microbiome influ-

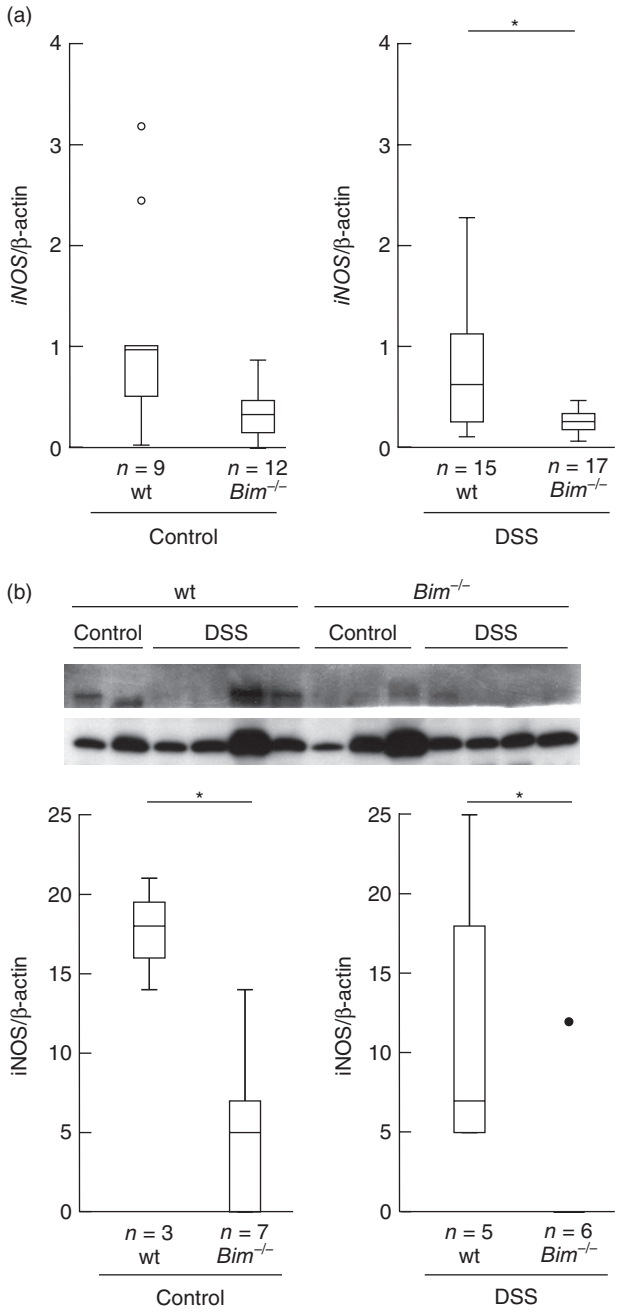

Fig. 5. Inducible nitric oxide synthase (iNOS) expression in whole Peyer's patches. (a) iNOS RNA expression. (b) iNOS protein expression.

ence prolapse development. However, our mice were housed in IVC in a SPF facility where a less developed microbiome could be expected.

We found significantly increased inflammation in *Bim*$^{-/-}$ animals compared to wild-type mice upon chronic DSS-induced colitis. The absence of Bim is the reason for an impaired removal of autoreactive TCR Vβ8^{+} lymphocytes in Peyer's patches upon chronic DSS-induced colitis. Conversely, an increase in Bim could have interesting consequences. Activation of Bim-mediated lymphocyte killing upon pro-apoptotic BH3-mimetics could adjust the balance between activated and regulatory lymphocyte populations and ameliorate colitis. Inducing apoptosis of autoreactive lymphocytes could be a new promising therapeutic strategy for CD patients.

Acknowledgements

This work was supported by the Swiss National Foundation (M.H., 31003A_127247) and the Broad Medical Research Program (M.H., IBD-0324R). We thank the microscopy centre at the University of Zurich (ZMB) for technical assistance.

Disclosure

K.L., M.K., M.F. and M.H. have no conflicts of interest to disclose. G.R. discloses grant support from Abbot, Ardeypharm, Essex, FALK, Flamentera, Novartis, Roche, Tillots, UCB and Zeller.

References

1 Puthalakath H, Huang DC, O'Reilly LA, King SM, Strasser A. The proapoptotic activity of the Bcl-2 family member Bim is regulated by interaction with the dynein motor complex. Mol Cell 1999; **3**:287–96.
2 Ley R, Ewings KE, Hadfield K, Cook SJ. Regulatory phosphorylation of Bim: sorting out the ERK from the JNK. Cell Death Differ 2005; **12**:1008–14.
3 Ewings KE, Wiggins CM, Cook SJ. Bim and the pro-survival Bcl-2 proteins: opposites attract, ERK repels. Cell Cycle 2007; **6**:2236–40.
4 Kutuk O, Letai A. Displacement of Bim by Bmf and Puma rather than increase in Bim level mediates paclitaxel-induced apoptosis in breast cancer cells. Cell Death Differ 2010; **17**:1624–35.
5 Ramjaun AR, Tomlinson S, Eddaoudi A, Downward J. Upregulation of two BH3-only proteins, Bmf and Bim, during TGF beta-induced apoptosis. Oncogene 2007; **26**:970–81.
6 Suzuki HI, Kiyono K, Miyazono K. Regulation of autophagy by transforming growth factor-beta (TGF-beta) signaling. Autophagy 2010; **6**:645–7.
7 Wojciechowski S, Tripathi P, Bourdeau T *et al.* Bim/Bcl-2 balance is critical for maintaining naive and memory T cell homeostasis. J Exp Med 2007; **204**:1665–75.
8 Bouillet P, Metcalf D, Huang DC *et al.* Proapoptotic Bcl-2 relative Bim required for certain apoptotic responses, leukocyte homeostasis, and to preclude autoimmunity. Science 1999; **286**:1735–8.
9 Tischner D, Woess C, Ottina E, Villunger A. Bcl-2-regulated cell death signalling in the prevention of autoimmunity. Cell Death Dis 2010; **1**:e48.
10 Mitchell T, Kappler J, Marrack P. Bystander virus infection prolongs activated T cell survival. J Immunol 1999; **162**:4527–35.
11 Hildeman DA, Zhu Y, Mitchell TC *et al.* Activated T cell death *in vivo* mediated by proapoptotic bcl-2 family member bim. Immunity 2002; **16**:759–67.

12 Bouillet P, Purton JF, Godfrey DI *et al.* BH3-only Bcl-2 family member Bim is required for apoptosis of autoreactive thymocytes. Nature 2002; **415**:922–6.
13 Tischner D, Gaggl I, Peschel I *et al.* Defective cell death signalling along the Bcl-2 regulated apoptosis pathway compromises Treg cell development and limits their functionality in mice. J Autoimmun 2012; **38**:59–69.
14 Atreya R, Mudter J, Finotto S *et al.* Blockade of interleukin 6 trans signaling suppresses T-cell resistance against apoptosis in chronic intestinal inflammation: evidence in crohn disease and experimental colitis in vivo. Nat Med 2000; **6**:583–8.
15 Boirivant M, Marini M, Di Felice G *et al.* Lamina propria T cells in Crohn's disease and other gastrointestinal inflammation show defective CD2 pathway-induced apoptosis. Gastroenterology 1999; **116**:557–65.
16 Ina K, Itoh J, Fukushima K *et al.* Resistance of Crohn's disease T cells to multiple apoptotic signals is associated with a Bcl-2/Bax mucosal imbalance. J Immunol 1999; **163**:1081–90.
17 Moret I, Rausell F, Iborra M *et al.* from DDW. Gastro supplement. Gastroenterology 2012; **142**:S-877.
18 Labi V, Erlacher M, Kiessling S *et al.* Loss of the BH3-only protein Bmf impairs B cell homeostasis and accelerates gamma irradiation-induced thymic lymphoma development. J Exp Med 2008; **205**:641–55.
19 Obermeier F, Kojouharoff G, Hans W, Scholmerich J, Gross V, Falk W. Interferon (IFN)-gamma- and tumour necrosis factor (TNF)-induced nitric oxide as toxic effector molecule in chronic dextran sulphate sodium (DSS)-induced colitis in mice. Clin Exp Immunol 1999; **116**:238–45.
20 Becker C, Fantini MC, Wirtz S *et al. In vivo* imaging of colitis and colon cancer development in mice using high resolution chromoendoscopy. Gut 2005; **54**:950–4.
21 Steidler L, Hans W, Schotte L *et al.* Treatment of murine colitis by *Lactococcus lactis* secreting interleukin-10. Science 2000; **289**:1352–5.
22 Hubner A, Cavanagh-Kyros J, Rincon M, Flavell RA, Davis RJ. Functional cooperation of the proapoptotic Bcl2 family proteins Bmf and Bim *in vivo*. Mol Cell Biol 2010; **30**:98–105.
23 Kruidenier L, Kuiper I, Van Duijn W *et al.* Imbalanced secondary mucosal antioxidant response in inflammatory bowel disease. J Pathol 2003; **201**:17–27.
24 Lu J, Wang A, Ansari S, Hershberg RM, McKay DM. Colonic bacterial superantigens evoke an inflammatory response and exaggerate disease in mice recovering from colitis. Gastroenterology 2003; **125**:1785–95.
25 Veltkamp C, Anstaett M, Wahl K *et al.* Apoptosis of regulatory T lymphocytes is increased in chronic inflammatory bowel disease and reversed by anti-TNFalpha treatment. Gut 2011; **60**:1345–53.